Potential phytoplankton responses to iron and stratification changes in the Southern Ocean based on a flexible-composition phytoplankton model

Mathieu Mongin, David L. Nelson, Philippe Pondaven, Paul Tréguer

Potential phytoplankton responses to iron and stratification changes in the Southern Ocean based on a flexible-composition phytoplankton model

Mathieu Mongin,[1] David M. Nelson,[2,3] Philippe Pondaven,[3] and Paul Tréguer[3]

[1] Under present climatic conditions, primary production in the Southern Ocean is limited by a combination of grazing pressure, the light/mixing regime, and iron. The response of the ecosystem to a permanent increase of iron supply and/or changes in the mixing regime is analyzed with a flexible-composition phytoplankton model that includes C, N, Si, and Fe cycling. Limitation of phytoplankton growth by light and nutrients (Si, N, and Fe) is treated through their effects on cellular elemental composition. The model is applied to the KERFIX time series in the subantarctic region. Two physical scenarios are considered, normal and reduced mixed layer depth, with four different aeolian inputs of Fe in each case ranging from 1 to 1000 times the estimated present input. These simulations suggest that Fe supply via dust and rain must be increased by more than a factor of 10 to produce significant changes. Increased Fe supply alone causes the bloom to occur later in the season (summer rather than spring), and coupled with a decrease in the mixed layer depth it produces drastic changes in the bloom intensity while preserving its present temporal development. Seasonal interaction between light and Fe limitation plays a critical role in controlling the primary and export production. If aeolian Fe input is increased by a factor of 1000, and mixed layer depth is reduced at the same time, export of carbon increases by a factor of 3. Light limitation prevents complete drawdown of nitrate, even if Fe limitation is removed and mixed layer depth reduced. This sets an upper limit on the primary production that can be achieved under the present meteorological conditions in this sector of the Southern Ocean.

Citation: Mongin, M., D. M. Nelson, P. Pondaven, and P. Tréguer (2007), Potential phytoplankton responses to iron and stratification changes in the Southern Ocean based on a flexible-composition phytoplankton model, *Global Biogeochem. Cycles*, *21*, GB4020, doi:10.1029/2007GB002972.

1. Introduction

1.1. HLNC Paradox

[2] One of the most important current questions in oceanic biogeochemistry is whether iron enrichment (either natural or anthropogenic) would increase oceanic primary productivity and associated drawdown of PCO_2, with possible implications for global climate change [*Martin*, 1990; *Falkowski et al.*, 1998]. Over the past decade, two major observations provide evidence that the Southern Ocean is key in that regard. First, Fe availability in Southern Ocean surface water is currently very low compared to other locations [*Blain et al.*, 2002]. Second, throughout the last glacial maximum, atmospheric pCO_2 was ∼50% lower than at present and more dust (and hence more Fe) was being delivered to the Antarctic [*Petit et al.*, 1999].

[3] Numerous studies over the past 15 years have shown that the possible controls on primary productivity in HNLC regions include micronutrient (especially Fe) availability, the light/mixing regime and grazing pressure [e.g., *Boyd et al.*, 2002; *Coale et al.*, 1996]. However, the relative strengths of those processes and their possible interactions are still debated [e.g., *Hiscock et al.*, 2003].

1.2. State of the Iron Hypothesis

[4] Several artificial Fe fertilization experiments have been conducted in the Southern Ocean to examine responses to increased [Fe] [e.g., *Boyd et al.*, 2000; *Coale et al.*, 2004]. The major result, both in the Southern Ocean and in other HNLC systems (reviewed by *De Baar et al.* [2005]) is that addition of Fe consistently stimulates phytoplankton growth, but after enrichment with Fe the light/mixing regime becomes the dominant process in controlling primary production. Unfortunately, during Fe fertilization

---

[1]Antarctic Climate and Ecosystem Cooperative Research Center, Hobart, Tasmania, Australia.
[2]College of Oceanic and Atmospheric Sciences, Oregon State University, Corvallis, Oregon, USA.
[3]Institut Universitaire Européen de la Mer-UMR CNRS 6539, Technopole Brest-Iroise, Plouzané, France.

experiments it has usually not been possible to follow the phytoplankton bloom over a period of time long enough to quantify any resulting change in carbon export fluxes. Only two (of the eight reported) studies followed Fe-induced blooms for long enough to evaluate carbon export: the Southern Ocean Fe Experiment (SoFex) [*Buesseler et al.*, 2005] and the Subarctic Ecosystem Response to Iron Enrichment Study (SERIES) in the subarctic Pacific [*Boyd et al.*, 2004].

[5] In reviewing the results of eight iron fertilization experiments in HNLC surface waters *De Baar et al.* [2005] concluded that the low-light environment that prevails in most parts of the Southern Ocean is responsible for the relatively small biogeochemical response to the increase of iron supply. This perspective was also suggested by *Coale et al.* [2004], who argued that lower wind stress during Fe enrichment experiment could lead to greater NO_3^- removal.

[6] In this context, modeling studies are useful because they can explore the ecosystem response to variations in Fe supply on timescales much longer than any field experiment can consider [*Gervais et al.*, 2002]. Some modeling studies have already explored the impact of temporal changes in Fe supply in the Southern Ocean [*Fennel et al.*, 2003; *Lancelot et al.*, 2000] and in the equatorial Pacific [*Jiang and Chai*, 2004]. Those models differ in the way they represent limitation of phytoplankton growth by light and nutrients. Some allow variation of the Si/N ratio as an empirical function of Fe limitation [*Blain et al.*, 2002; *Aumont et al.*, 2003; *Moore et al.*, 2002]. For our model, we chose a physiologically based approach, using what we believe to be the most realistic formulation of the cellular processes associated with Fe uptake and growth.

2. Model Description

[7] The model [*Mongin et al.*, 2006] is one-dimensional, covering the upper 400 m of the water column with a layer thickness of 5 m. Time courses of temperature and vertical mixing are simulated using a turbulent kinetic energy (TKE) parameterization [*Gaspar et al.*, 1990]. The model is forced using sea surface wind stress, short-wave radiation and long-wave radiation for the French Kerguelen Point Fixe (KERFIX) site in the Indian sector of the Southern Ocean (50.7°S, 68.4°E) over the 1989–1994 period, taken from the European Centre for Medium-Range Weather Forecasting (ECMWF). The model is run for 5 years (with a 4 year spin-up); hence results presented here are for the 1993–1994 period.

[8] The biogeochemical model contains two phytoplankton groups (diatoms and small nonsiliceous forms), two size classes of zooplankton (micro- and mesozooplankton), heterotrophic bacteria, two detritus pools (large and small particles), and two dissolved organic matter pools (labile and semilabile). The model allows the uptake of NO_3^-, NH_4^+, $Si(OH)_4$ and biologically available iron (Fe_B) and the photosynthetic fixation of C to be independent of one another within a constrained range of elemental ratios as proposed by the Droop cell quota model [*Droop*, 1974, 2003]. All nutrient uptake is biological and no inorganic

scavenging of Fe is included. When the Fe cell quota (as represented by the phytoplankton Fe/C ratio) reaches low values, photosynthetic efficiency (the initial slope, α, of a photosynthesis-irradiance curve) and the maximum rate of NO_3^- uptake decrease following Droop's model, reaching zero at the lowest cellular Fe/C ratio permitted (1.5×10^{-6} mol/mol). Figure 1 shows the Droop model with α and the maximum rates of NO_3^- and Fe uptake as a function of the cellular Fe/C ratio. Exactly analogous controls simulate $Si(OH)_4$ uptake, (with Si/N ratio used as a proxy for Si cellular quota), photosynthesis (through the C/N ratio) and uptake of NO_3^- and NH_4^+ (using Si/N and C/N ratios). Overall, this dual control (external concentration and internal composition) allows more flexibility in the nutrient uptake and photosynthesis as elemental ratios can reduce the rate of nutrient uptake even if there is plenty of that nutrient (or light) available.

[9] Light penetration through the upper water column is based upon the spectral irradiance model of *Morel* [1991]. Attenuation is set using chlorophyll and particulate organic matter concentration within the water column. Photosynthetically available radiation (PAR) decreases with depth in response to this attenuation, but is calculated as a mean over the mixed layer to take account of the low-light cellular adaptation time under rapid vertical mixing [*Anderson*, 1993]. When no macronutrient (N or Si) limits phytoplankton growth rates irradiance controls the photosynthetic rate through a light limitation term, $LE = 1 - e^{\frac{-\alpha*PAR}{mumax}}$; the cellular Fe/C ratio controls via a Droop cell quota formulation, hence allowing colimitation of photosynthesis by Fe and light. Irradiance also modifies the maximum rate of NO_3^- uptake via a similar LE term.

[10] $[NO_3^-]$, $[Si(OH)_4]$ and $[Fe_B]$ are restored to full vertical data profiles between 1 July and 1 September of each year. This restoration procedure simulates northward advection of nutrients in winter [*Mongin et al.*, 2006]. Deep iron concentrations are set assuming a constant Fe_B/NO_3^- ratio of 1×10^{-5}, causing any vertical exchange to supply Fe_B at 1×10^{-5} times the rate at which it supplies nitrate. This Fe_B/NO_3^- ratio is slightly higher that the 3×10^{-6} estimated value by *Fung et al.* [2000]. Removal of phytoplankton Fe by grazing is calculated as the ingestion rate of phytoplankton C multiplied by the Fe/C ratio of the phytoplankton. All Fe ingested by the zooplankton is rejected into the detritus pool as fecal pellets. The specific rates of both N and Fe regeneration from detritus are set at 0.05 d^{-1} for diatom-derived detritus and 0.07 d^{-1} for the detritus from nonsiliceous phytoplankton.

[11] The first application of a model of this type was at the Bermuda Atlantic Time-series Study (BATS) site in the western Sargasso Sea [*Mongin et al.*, 2003], where the Droop formulation, the evolution of elemental ratios, and the microbial loop parameterization were validated. More recently we have incorporated a Fe cycle and Fe limitation into this model and applied it at the KERFIX site [*Mongin et al.*, 2006]. Using present-day annual estimates of aeolian dissolved Fe inputs (based on Southern Ocean regional estimates proposed by *Gao et al.* [2003]), the model reproduces the observed HNLC condition around KERFIX. Fe limitation controls the timing (beginning and
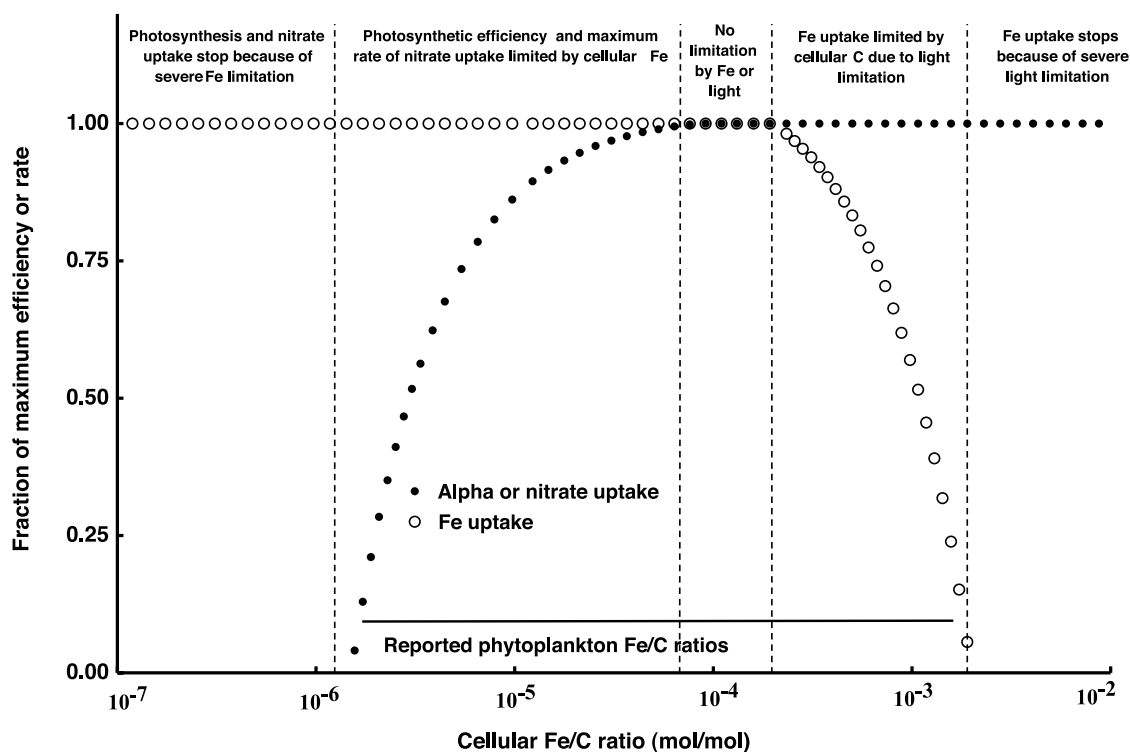
Figure 1. Fraction of the maximum photosynthetic efficiency (initial slope, α, of a photosynthesis: irradiance curve) and rate of nitrate uptake as a function of the cellular Fe/C mole ratio of phytoplankton. Curves shown represent *Droop*'s [1974] cell quota function. Approximate range of cellular Fe/C ratios reported for phytoplankton in culture studies is also shown.

length) of the spring bloom and causes low productivity in summer. Grazing controls the maximum phytoplankton biomass than can develop during the bloom. Light limitation interacts with Fe limitation, resulting in low photosynthetic rates in winter because of low solar irradiance and in summer because the low cellular Fe/C ratios impose low photosynthetic efficiency. Those results imply that neither grazing pressure, Fe limitation nor light limitation taken alone can explain the persistence of HNLC conditions through the summer. In the study reported here we use the same model to explore the response of the ecosystem around the KERFIX site to (1) changes in aeolian inputs of Fe from dust and rain and (2) light/mixing conditions more favorable for photosynthesis.

[12] The aeolian inputs of dissolved Fe are set to 1.5 mg (26.8 μmol) Fe m^{-2} a^{-1} in the base simulation, and are increased to 15 mg (268 μmol) Fe m^{-2} a^{-1}, 150 mg (2.68 10^3 μmol) Fe m^{-2} a^{-1} and 1,500 mg (2.68 10^4 μmol) Fe m^{-2} a^{-1} in the dust experiments. These annual inputs range from approximately the present rate for the Southern Ocean [*Gao et al.*, 2003] to ∼1000 times the present rate and approximately that estimated for the Southern Ocean during the last glacial maximum [*Martin*, 1990]. All dissolved Fe delivered is considered to be biologically available and no seasonality is imposed on the aeolian Fe$_B$ input in these simulations.

[13] For each experiment, two physical scenarios were considered. In the first (Case 1) the original meteorological

forcing (ECMWF, 1989–1995 period) leads to a realistic simulation of the temperature and mixing for the KERFIX site [*Mongin et al.*, 2006]. The second (Case 2) with wind stress values artificially reduced by a factor 3 (i.e., possible reduction caused by global warming, [*Matear and Hirst*, 2003]), leads to a realistic simulation of the sea surface temperature, but mixing is attenuated (see Figure 2).

3. Results

[14] Six simulations are presented: three for the Case 1; referred as "Dust*1", "Dust*100" and "Dust*1000", and three for Case 2; referred as "Dust*1b", "Dust*100b" and "Dust*1000b". Model results are presented as mixed layer means for the 1993–1994 season (chosen upon its representation of the 1989–1995 inter annual cycle). Annual biogeochemical fluxes (Table 1) are presented as depth-integrated values for the upper 200 m. Results obtained with 10 times the present dust input are almost indistinguishable from those the present dust input and therefore are not shown. This occurs because the present rate (1.5 mg Fe m^{-2} a^{-1}) is much lower than the rate of supply by advection and vertical mixing, and accounts for only 2.5% of the annual Fe uptake by phytoplankton.

3.1. Chlorophyll-a

[15] Time courses of chlorophyll-a (Chl-a) are presented in Figures 2a and 2b. In the Case 1 simulation increasing the aeolian Fe supply by a factor 100 produces significant
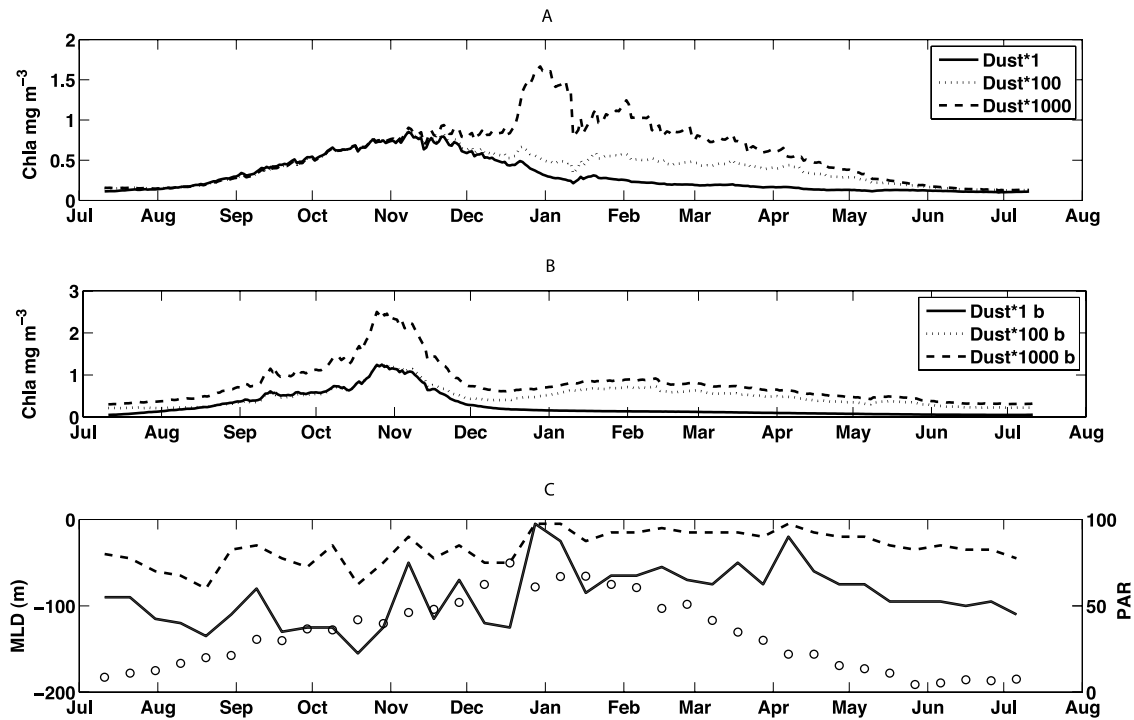
Figure 2. Time courses of chlorophyll-*a* (mg m^{-3}) treated as a mean over the mixed layer for three different Fe dust inputs: (a) KERFIX based mixed layer. (b) Reduced mixed layer. (solid line) Present time Fe Dust. (dotted line) Fe Dust*100. (dashed line) Fe Dust*1000. (c) Mixed layer depth (in meters) left axis. (solid line) KERFIX based mixed layer. (dashed line) Reduced mixed layer. (right axis, dots) Model 24-h mean photosynthetically available radiation (PAR) in the surface mixed layer (μE m^{-2} s^{-1}).

changes in "Chl-a (higher concentration during autumn compared to "Dust*1"). Increasing Fe supply by a factor 1000 increases the maximum Chl-a concentration in surface waters by about a factor of 2 over that attained in "Dust*1" (~1.7 versus ~0.8 mg m^{-3}). At the highest-dust input, the maximum bloom intensity occurs later in the year (December/January, versus November in the "Dust*1" simulation) and coincides with the maximum solar irradiance in the upper mixed layer (Figure 2c). The effect of a reduced mixed layer (Case 2, Figure 2b), while supplying the same amount of nutrient into the upper ocean during winter because of restoration, has more drastic effect on Chl-a during the bloom period than in Case 1, with a Chl-a

maximum reaching 2.4 mg m^{-3} in the "Dust*1000b" simulation in November. The impact of increased dust input is somewhat stronger than in Case 1 (maximum Chl-a of ~2.4 mg m^{-3} versus ~1.7 mg m^{-3} in the "Dust*1000" simulations), but the bloom maximum does not shift later in the season as it does at "Dust*1000" in Case 1.

3.2. Nutrients

[16] Case 1 nitrate concentration [NO$_3^-$] (Figure 3a) shows a response to aeolian Fe input similar to that of Chl-a. The major difference in response to Fe is between the "Dust *100" and "Dust *1000" simulations where mid-summer minimum in [NO$_3^-$] is ~4 μM lower at the greatest

Table 1. Annual Fluxes of C, N, and Si Predicted by the Model for the Six Simulations Presented as 4-Year (a) Means, 11 July 1992 Through 10 July 1996

|	Case 1			Case 2		
	Dust *1	Dust *100	Dust *1000	Dust *1	Dust *100	Dust *1000
Primary productivity, mol C m^{-2} a^{-1}	5.6	7.6	12.8	4.3	6.8	17.4
Organic N production, mol N m^{-2} a^{-1}	1.5	2.0	3.2	1.2	1.7	3.15
Biogenic SiO$_2$ production, mol Si m^{-2} a^{-1}	3.6	4.2	4.2	2.8	3.1	1.7
Diatom productivity, mol C m^{-2} a^{-1}, % of total	3.1 (56.0%)	4.1 (54.6%)	7.0 (55.0%)	2.5 (55.8%)	3.8 (55.9%)	1.9 (10.0%)
Nonsiliceous productivity, mol C m^{-2} a^{-1}, % of total	2.5 (44.0%)	3.5 (45.4%)	5.8 (45%)	1.8 (44.2%)	3.0 (44.1%)	15.5 (90.0%)
Diatom Fe/C ratio, μmol Fe/mol C	77.5	92.3	174.3	41.5	54.5	112
POC export at 200 m, mol C m^{-2} a^{-1}, % of productivity	1.9 (33.8%)	2.5 (32.8%)	4.9 (31.8%)	1.5 (34.8%)	2.2 (32.4%)	4.6 (26.4%)
Biogenic SiO$_2$ export at 200 m, mol Si m^{-2} a^{-1}	2.3	2.7	2.8	1.7	1.9	1.2
C/N export ratio, mol/mol	6.9	7.2	7.9	7.1	7.9	10.2
Si/N export ratio, mol/mol	8.3	7.8	5.4	8.1	6.8	2.3
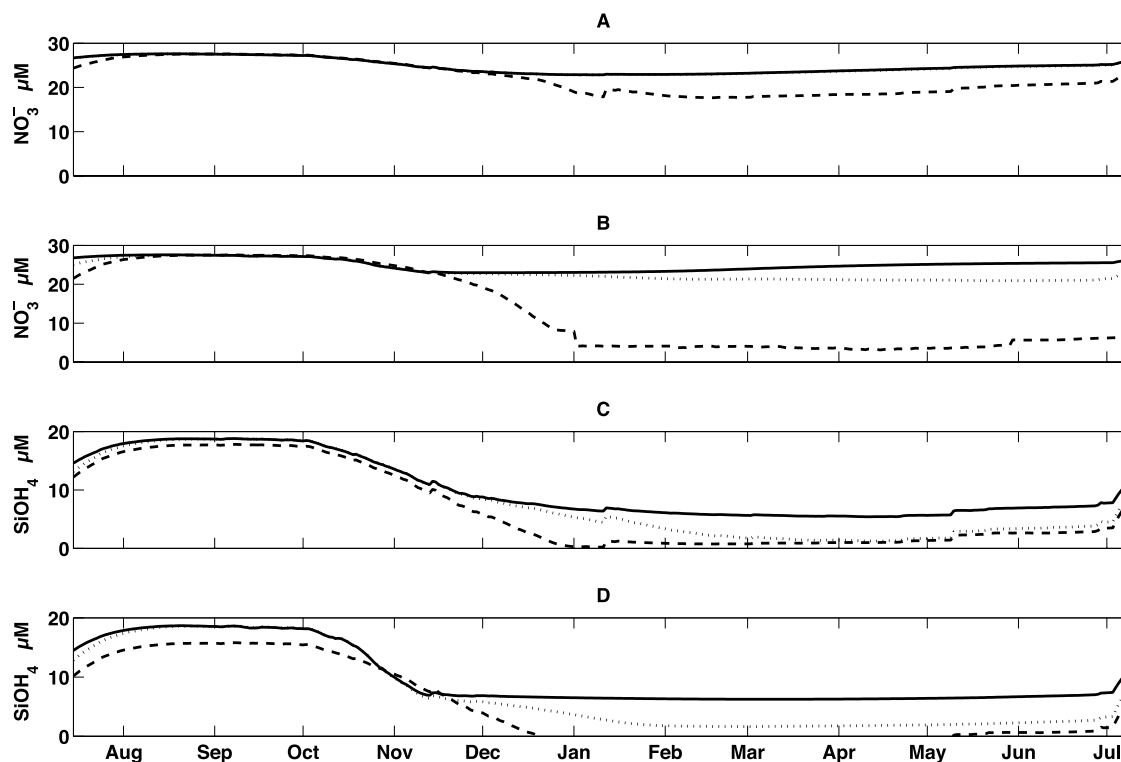
Figure 3. Time courses of [NO_3^-] (μM): (a) KERFIX mixed layer. (b) Reduced mixed layer. Time courses of [$Si(OH)_4$] (μM): (c) KERFIX mixed layer. (d) Reduced mixed layer. (solid line) Present time Fe Dust. (dotted line) Dust*100, (dashed line) Dust*1000.

dust input considered. However, even in "Dust*1000" considerable unused NO_3^- remains in the upper water column, with mean [NO_3^-] in the mixed layer >15 μM. On the other hand, in the Case 2 ("Dust * 1000b", Figure 3b), summer nitrate depletion is more severe with [NO_3^-] as low as 5 μM.

[17] The time course of [$Si(OH)_4$] shows a response to increased aeolian Fe input very different from that of [NO_3^-] (Figure 3c). It is still necessary to increase the aeolian supply by a factor of 100 to stimulate significant changes, but at the highest-Fe input considered the minimum [$Si(OH)_4$] is much lower than [NO_3^-] (<1 μM versus >15 μM). Summer [$Si(OH)_4$] levels of 7–8 μM observed in the "Dust*1" simulation would be nonlimiting or only weakly limiting to most Southern Ocean diatom assemblages, but the <1 μM levels that persist through the summer at the highest-Fe inputs would be strongly limiting [*Nelson et al.*, 2001]. As is the case for [NO_3^-], [$Si(OH)_4$] is depleted much more rapidly in Case 2 (Figure 3d), with values as low as ~1 μM in the Dust*100 b simulation.

[18] In the Case 1 simulations [Fe_B] reaches an annual maximum of ~0.25 nM in mid-August in Dust*1 and Dust*10 (Figure 4a). That maximum is due to the combined effects of the constant [Fe_B]/[NO_3^-] mole ratio of 1×10^{-5} in deep water, the restoration to the KERFIX nutrient data in winter, and the strongly seasonal uptake of NO_3^- and Fe by phytoplankton. Surprisingly the winter maximum in [Fe_B] is lower in "Dust*100" and "Dust*1000" than in "Dust*1",

reaching maximum values of 0.2 and 0.12 nM, respectively. This results from the combined effects of the greater photosynthetic efficiency and higher-phytoplankton biomass during winter, which result in greater uptake of Fe by phytoplankton during winter. Although the winter maximum [Fe_B] is lower in the simulation with the greatest dust input, that high-dust input causes considerably more Fe to remain in the mixed layer through the summer. In the simulations at 1000 times the present dust input, mixed layer [Fe_B] ranges only from 0.05 nM in summer to 0.12 nM in winter (Figures 4a and 4b). Thus in these simulations the increased aeolian supply removes much of the seasonal variability in [Fe_B], keeping Fe available at reasonable concentrations throughout the year. The impact of a reduced mixed layer (Case 2 simulations) has little effect on [Fe_B] (Figure 4b) as the winter supply stays essentially the same.

3.3. Phytoplankton Elemental Ratios

[19] At 1 and 10 times the current aeolian Fe input, diatom Si/N ratios remain ~4.0 (mol/mol) at all times of year (Figure 5). This is much higher than the 1.0 value characteristic of Fe-replete diatoms [*Brzezinski*, 1985; *Hutchins and Bruland*, 1998; *Takeda*, 1998]. In the model this high-Si/N ratio is also a consequence of Fe limitation, which reduces photosynthetic efficiency and the maximum rate of nitrate uptake but has no direct effect on Si uptake. At 100 times the present aeolian input, diatom Si/N ratios decrease to ~1.5 in autumn (April), reflecting the fact that
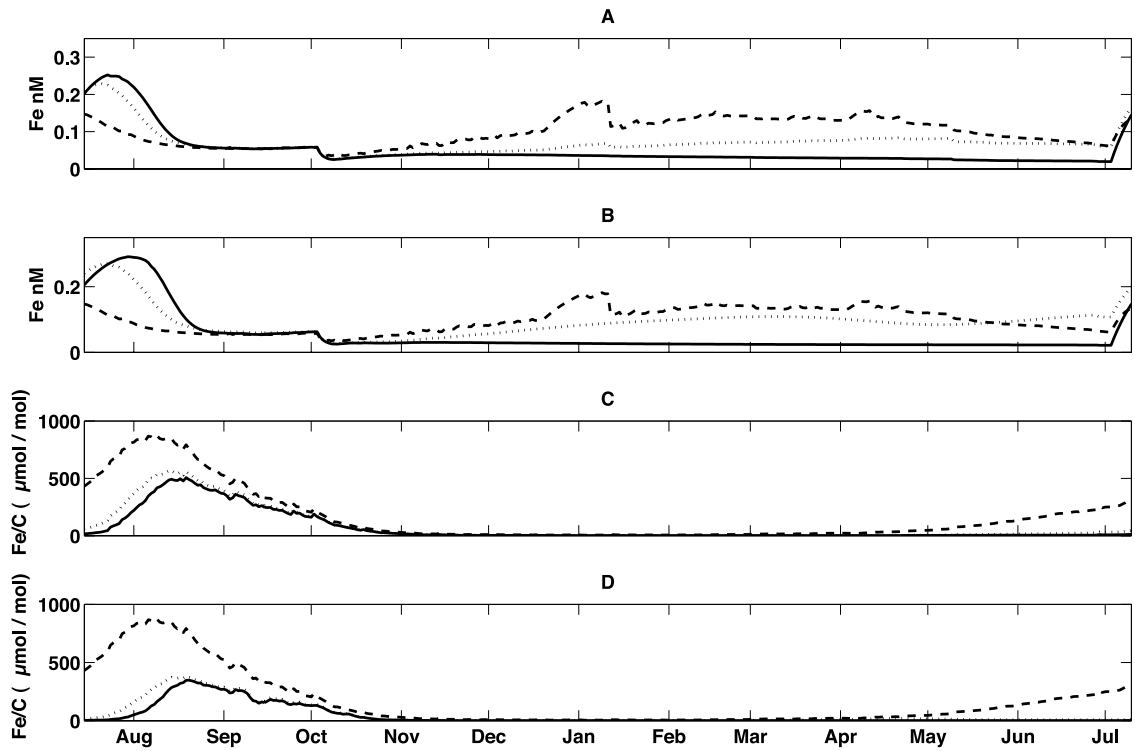
Figure 4. Time course of biologically available iron [Fe$_B$] (μM): (a) KERFIX mixed layer. (b) Reduced mixed layer. Time course of mean mixed layer diatom Fe/C ratio (μmol Fe/mol C): (c) KERFIX mixed layer. (d) Reduced mixed layer. (solid line) Present time Fe Dust. (dotted line) Dust*100. (dashed line) Dust*1000.
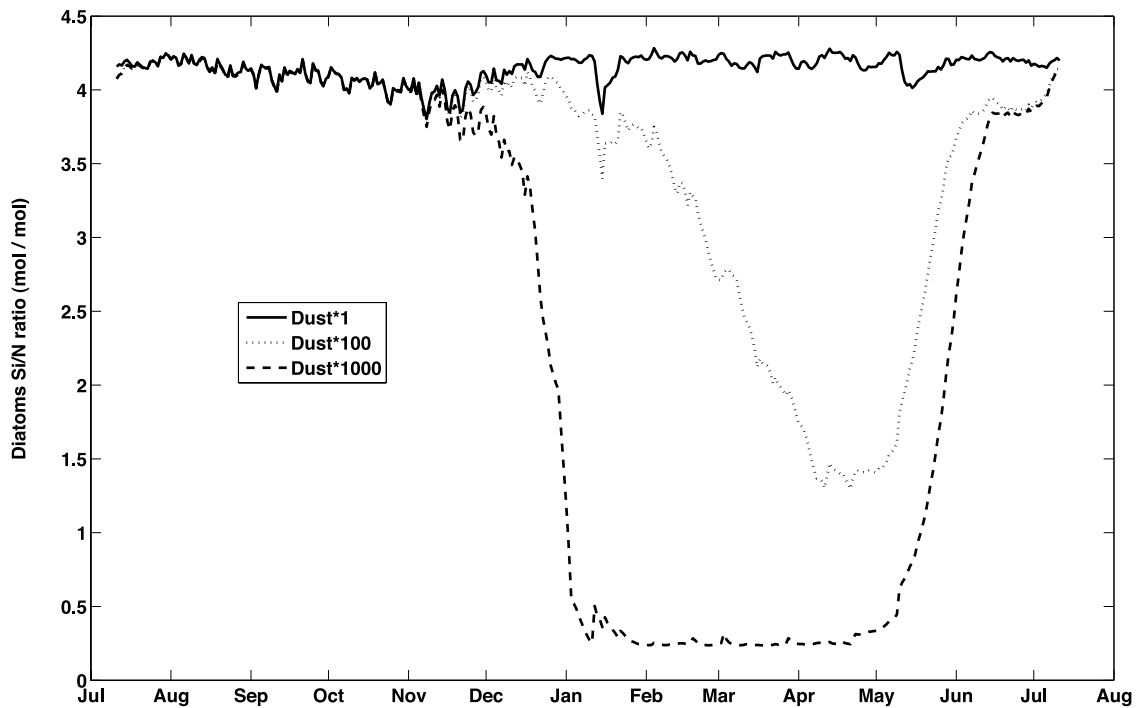

Figure 5. Diatom Si/N ratio (mol/mol) time course for the three simulations with the KERFIX mixed layer. (solid line) Present time Fe Dust. (dotted line) Dust*100. (dashed line) Dust*1000.
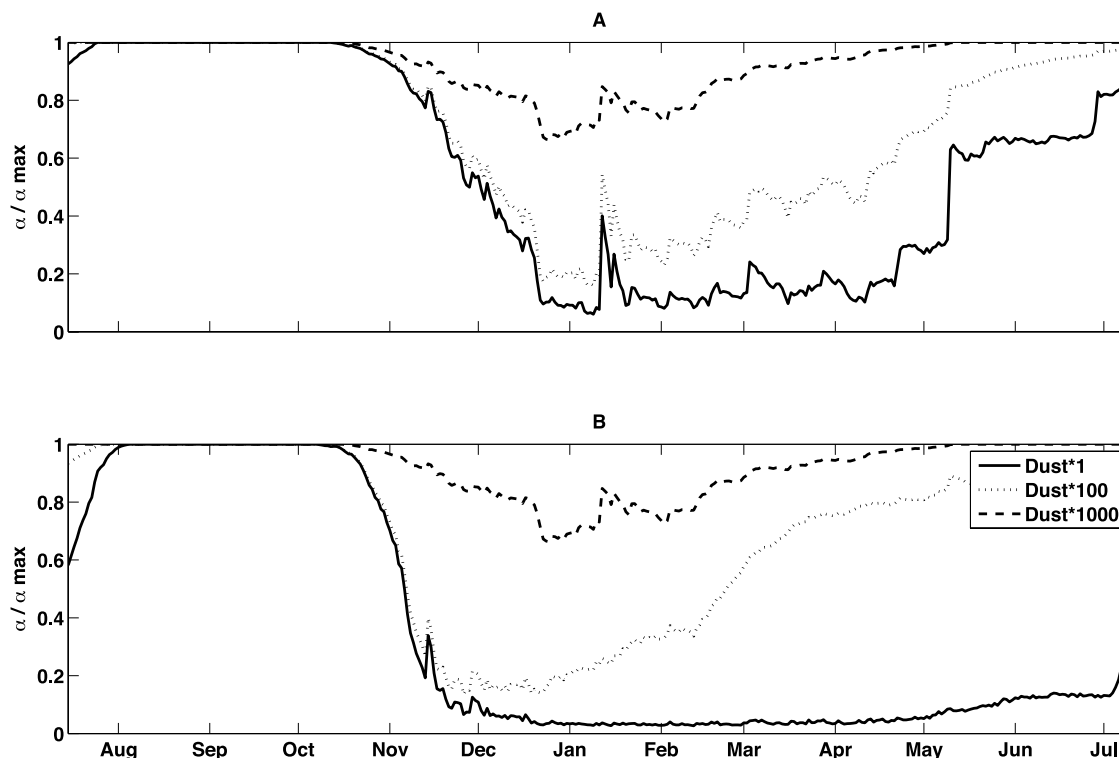
Figure 6. Relative photosynthetic efficiency (α/α_{max}), an unambiguous index of the severity of Fe limitation in the model. (a) KERFIX mixed layer. (b) Reduced mixed layer. (solid line) Present time Fe Dust. (dotted line) Dust*100. (dashed line) Dust*1000.

Fe limitation is weaker (and maximum rates of nitrate uptake therefore higher). At 1000 times the present aeolian Fe input, diatom Si/N ratios remain <0.5 throughout the stratified period (January–April) with a minimum value of ~0.2. Those low-diatom Si/N ratios are a direct consequence of the strong surface depletion of [Si(OH)$_4$] that occurs when Fe is supplied at higher rates. Under those conditions, diatom growth, NO$_3^-$ uptake and photosynthesis are controlled by Si limitation through much of the summer.

[20] The annual mean diatom Fe/C ratio under the current aeolian Fe input (Case 1) is 77 μmol Fe/mol C, equivalent to ~13,000 atoms of carbon fixed for each atom of Fe taken up (Table 1). This value can be compared to the value of 20,000 from *Lancelot et al.* [2000] and 15,000 from the open ocean Fe fertilization experiments [*De Baar et al.*, 2005]. Diatom Fe/C ratios range from 6.6 to 700 μmol/mol in "Dust*1000" and from 2 to 500 μmol/mol in the other simulations (see Figure 4c). In the Case 2 simulations, where light is less limiting because of the decreased mixed layer depth, photosynthesis is greater for the same amount of Fe taken up, so the phytoplankton Fe/C ratio slightly decreases under the greater Fe$_B$ supply (380 μmol/mol in Dust*100b and 550 μmol/mol in Dust*100a; see Figure 4d). These results are similar to those obtained in diatom culture experiments [*Strzepek and Price*, 2000], where Fe/C ratios go down as irradiance increases (Fe/C range: 20–500 μmol/mol).

[21] In the model the initial slope of the photosynthesis-irradiance curve (α) is affected only by the cellular Fe/C ratio of the phytoplankton, which in turn responds to changes in [Fe$_B$]. The ratio α/α_{max} (where α_{max} is a constant imposed value reflecting the photosynthetic efficiency of Fe-replete cells) therefore provides an unambiguous measure of the severity of Fe limitation in each simulation. Time courses of α/α_{max} under Case 1 (present mixed layer depths) and Case 2 (reduced mixing) conditions are shown in Figure 6. At all assumed aeolian Fe inputs α/α_{max} is ~1.0 in late winter, indicating Fe sufficiency. At the present dust input α/α_{max} decreases to <0.1 through most of the summer, indicating very severe Fe limitation of phytoplankton photosynthesis and nitrate uptake. However, at 100 times the present aeolian input, Fe limitation is somewhat less severe (annual minimum α/α_{max} ~0.2) and increases much more in autumn (March and April) than it does at present dust inputs. At 1000 times the present input, only brief and minor Fe limitation is observed (annual minimum α/α_{max} ~0.7) indicating almost complete elimination of Fe-limited conditions for the phytoplankton.

3.4. Annual Fluxes

[22] The annual fluxes obtained in these simulations are reported in Table 1. Primary productivity increases by a factor of 2 in response to a 1000-fold increase in aeolian Fe input under present mixing conditions (Case 1), and by a factor of 4 with significantly reduced mixing (Case 2). In all "Dust*1" and "Dust*100" simulations annual primary productivity is still <100 g C m^{-2} a^{-1}, similar to that
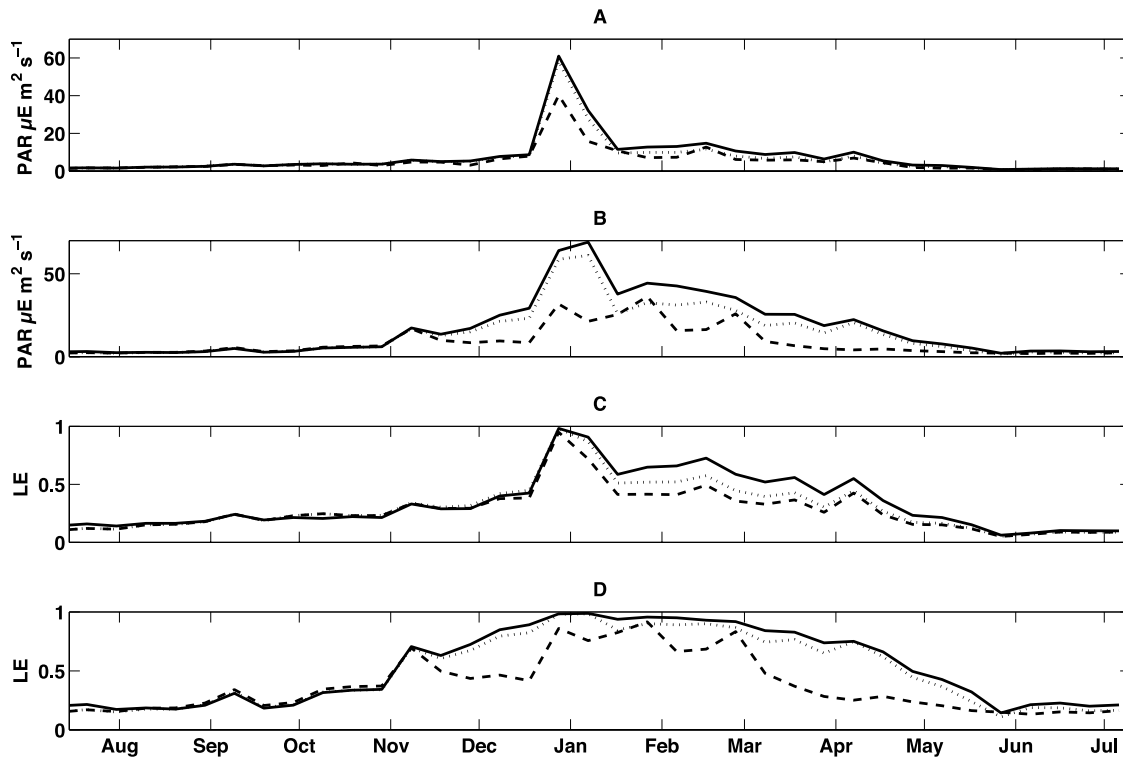
Figure 7. Daily photosynthetically available radiations (PAR). (a) KERFIX mixed layer. (b) Reduced mixed layer. Light limitation term (LE = $1 - e^{-\alpha_{max}\ PAR/\mu_{max}}$) with α_{max} not affected by Fe, see text for details. (c) KERFIX mixed layer. (d) Reduced mixed layer. (solid line) Present time Fe Dust. (dotted line) Dust*100, (dashed line) Dust*1000.

estimated from ^{14}C uptake [e.g., *Nelson et al.*, 2002] and lower than that in the oligotrophic subtropical gyres [e.g., *Michaels et al.*, 1994]. Under present mixing conditions (Case 1) biogenic silica production also increases under higher-Fe dust input, but only from 3.6 to 4.2 mol Si m^{-2} a^{-1}. Carbon export due to particles sinking at 200 m more than doubles between the "Dust*1" and "Dust*1000" simulations (from 1.9 to 4.9 mol C m^{-2} a^{-1}) while biogenic silica export increases only from 2.3 to 2.8 mol Si m^{-2} a^{-1}. A shallower mixed layer depth (Case 2 simulations) does not result in greater export of either POC or biogenic SiO$_2$. POC export remains sensitive to aeolian Fe input, being 3 times as high in the "Dust*1000b" simulations as at "Dust*1b" (4.6 versus 1.5 mol C m^{-2} a^{-1}) This increase in carbon export is consistent with results obtained with other model studies [*Fennel et al.*, 2003; *Moore et al.*, 2002] and proves to be a robust result, relatively independent of the model structure and/or calibration.

3.5. Light Penetration and Limitation

[23] The time course of PAR, vertically averaged over the mixed layer, is presented in Figures 7a and 7b. It ranges from $60-70$ μE m^{-2} s^{-1} in December to <10 μE m^{-2} s^{-1} in June in the Case 1 simulation, and is somewhat attenuated when mixing is reduced (Case 2) because of the higher-chlorophyll-a content (see Figure 2). Mixed layer average PAR does not show major differences among the six

simulations from May through early December; this is a consequence of low chlorophyll, low surface irradiance, and deep mixing in winter (May through September) and increasing chlorophyll-a in the mixed layer in spring (October through early December). In summer PAR is further reduced when dust inputs increase, a consequence of the higher-chlorophyll levels attained when Fe limitation is less severe. There is only a brief period near the solar maximum in December when the mean PAR in the upper mixed layer is >15 μE m^{-2} s^{-1}. That level corresponds to an integrated daily irradiance of ~1.3 E m^{-2} d^{-1}, approximately equal to the net photocompensation irradiance estimated by *Siegel et al.* [2002] for the North Atlantic. In Siegel's study, the net photocompensation irradiance represents the light level at which phytoplankton photosynthesis just balances the sum of all phytoplankton removal terms, resulting in a net phytoplankton growth rate of zero. As such it represents a severely light-limited condition. The fact that the mean PAR in the mixed layer is <15 μE m^{-2} s^{-1} throughout most of the summer growing season at all Fe inputs shows that in these simulations the maximum attainable chlorophyll levels are strongly controlled by low PAR in the upper mixed layer, regardless of the aeolian Fe supply.

[24] We can define a pure light limitation term (LE = $1 - e^{-\alpha_{max}\ PAR/\mu_{max}}$). This is the same light limitation term described earlier, but with α replaced by α_{max} and thus not affected by Fe limitation. That term, shown in
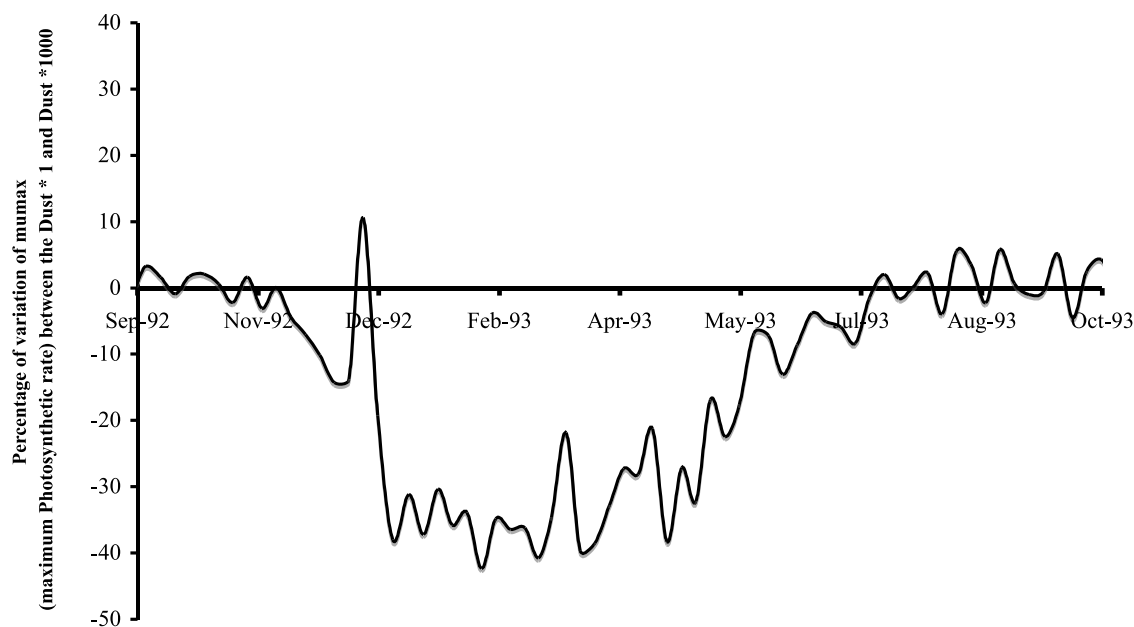
Figure 8. Percentage of variation of μ_{max} (maximum photosynthetic rate) between the simulations at 1 and 1000 times the present aeolian Fe input, using the KERFIX mixed layer.

Figures 7c and 7d, displays the degree of light limitation affected only by irradiance and not by Fe. It is clear that, even if [Fe$_B$] were never low enough to make $\alpha < \alpha_{max}$, primary production around the KERFIX location would be strongly light limited because of low surface irradiance, except during a short period around midsummer. The difference between the different dust input simulations also shows increased light limitation as Fe limitation weakens. This is a consequence of increased chlorophyll in the mixed layer. To quantify the influence of this decreased light availability on photosynthesis at the highest-Fe input in comparison with the lowest-Fe input, we calculate the variation of the maximum photosynthetic rate influenced by the ambient PAR only (Figure 8). This calculation is based on the light limitation term considering a constant photosynthesis-irradiance curve (not modified by the low [Fe$_B$]). As such, it ignores the direct effect of Fe limitation and considers light limitation alone (arising from the decrease of light penetration between the "Dust*1" and "Dust*1000" simulations). At high-Fe input, self-shading decreases chlorophyll-specific photosynthetic rates in the mixed layer by a factor of 2 in comparison with those attainable at low-Fe input. This means that in these simulations the greater photosynthetic efficiency that persists through the summer at high-Fe inputs (Figure 6) is offset to a significant degree by the lower mean surface layer PAR that results from higher-chlorophyll concentrations within the mixed layer.

4. Discussion

[25] While our model addresses *Martin*'s [1990] iron hypothesis to some degree, by investigating phytoplankton responses to aeolian Fe inputs greater than those that are observed at present, we do not report these model results

as simulations of the glacial Southern Ocean or a test of that hypothesis. Simulating the true "glacial" scenario would require access to the meteorological condition at that time, along with a full understanding of the processes that control iron concentrations in deep water. That is why we report our result as a nonglacial scenario. Because the processes involved are numerous and complex, they cannot be tested realistically all at once. Models are just the right tools to explore a situation of that kind as we can easily separate processes and examine the influence of each process independently.

[26] The purpose of these simulations is simply to assess the ecosystem response to a permanent increase in the aeolian supply of Fe with or without reduced mixing. Dust input to the ocean is known to be highly variable both spatially and temporally [e.g., *Gao et al.*, 2003]. In the simulations reported here we chose to deliver aeolian Fe at a constant rate throughout the year; temporal variability in Fe$_B$ inputs can be added in future simulations. Additionally our model does not address the impact of increased aeolian Fe input on the Fe/NO$_3^-$ ratio of the deep ocean. A further simulation (not shown) reveals that if subsurface Fe$_B$ is not held constant but artificially increased by 50%, along with a 10-fold increase in aeolian input, annual primary production, which is increased by 11% at "Dust*10" is increased by 16%. This additional test shows that one key to understanding the Southern Ocean's response to variations in dust input is the response (or lack thereof) of the subsurface iron pools, as most iron comes from below in any given year. Our results are therefore dependent on this assumed lack of response of the Fe/NO$_3^-$ ratio of the deep ocean to dust inputs.

[27] The value of the present aeolian Fe$_B$ dust input used here, while we consider it to be the best estimate currently available, contains many uncertainties (e.g., transport,

solubility of Fe). Other constraints come from the fact that the model is calibrated for the KERFIX time series. This location (the only long-term sampling location yet occupied in the Southern Ocean) may be representative of the HNLC conditions in much of the permanently ice-free Southern Ocean. However, these results exclude the sea ice zone (where light limitation should be stronger and more persistent seasonally because of seasonal ice cover) and a vast area south of the Antarctic Polar Front where late winter $[Si(OH)_4]$ is higher and diatoms could therefore grow to greater abundance before encountering Si limitation [*Nelson et al.*, 2001]. Finally, we focused our attention on the Southern Ocean, which is well known for its low-dust input and relatively high rate of Fe supply from below by upwelling and mixing. Phytoplankton responses to a 10-fold increase of dust in other basins such as the southwest Atlantic or subarctic Pacific would likely be much higher.

[28] Despite these constraints, the simulations reported here imply that primary production in the Southern Ocean is limited by the interacting effects of Fe limitation and light limitation, much as predicted by *Sunda and Huntsman* [1997]. That result is very robust, occurring at all dust inputs and under both vertical-mixing scenarios. Our simulations therefore yield the following predictions for a Southern Ocean in which the aeolian Fe supply is 100–1000 times higher than it is at present:

[29] 1. A 100-fold increase in aeolian Fe supply diminishes Fe limitation significantly and 1000-fold increase all but eliminates Fe limitation in the system.

[30] 2. There is a clear seasonal oscillation between Fe limitation and light limitation in this part of the Southern Ocean, with light limitation dominant in winter and Fe limitation in summer; as a consequence, an increased aeolian Fe supply produces a much stronger signal when coupled with decreased mixing (and hence increased light availability in the upper mixed layer).

[31] 3. Annual primary productivity and POC export can increase by a little more than a factor of 2 with aeolian Fe inputs high enough to eliminate Fe limitation. If mixing were to be reduced at the same time, the increase could rise to about a factor of 3.

[32] 4. Under increased aeolian Fe supply $[Si(OH)_4]$ would be depleted in summer to levels that strongly limit biogenic silica production and diatom growth.

[33] 5. Phytoplankton uptake would not deplete $[NO_3^-]$ to limiting levels, even when Fe limitation is eliminated by increased dust supply and vertical mixing is reduced.

[34] 6. The amount of chlorophyll produced with a higher-Fe supply would reduce the light penetration in the water column to a degree that would cause the chlorophyll-specific photosynthetic rate to be reduced 50% by self-shading.

[35] While both an increase in Fe supply and a more favorable light/mixing conditions enhance the phytoplankton bloom, their effects on the bloom's seasonality are different. Increasing the Fe supply alone pushes the bloom to occur later in the season (when the solar irradiance is maximum). On the other hand, a more favorable light/mixing regime, either alone or with increased Fe, supply

does not alter the seasonality of primary production. This implies that under present conditions, the bloom at the KERFIX site is more light-limited than Fe-limited. Moreover it shows that light is (more so than Fe) the major factor controlling bloom strength.

[36] Results obtained from model simulations of the Southern Ocean north of the Antarctic Polar Front [*Fennel et al.*, 2003; *Moore et al.*, 2002] also suggest this light/Fe seasonal pattern. In those simulations, primary production and export increased by about a factor of 2 when Fe limitation was eliminated, similar to the results obtained here. Our results, obtained using different, and we believe physiologically more realistic, functions to relate photosynthesis and nutrient uptake to cellular elemental composition, yield similar results for export. This suggests that the approximate doubling in primary productivity obtained in all simulations is a relatively robust result, not highly dependent on model structure or the formulation of specific processes.

[37] Comparison of the model results with those from experimental iron fertilization studies is not a straightforward task, as the model was not built specifically to address those experiments. In our simulations iron "fertilization" is done at every time step of the run throughout the year; thus the biological response is different from the one obtained with a short-term fertilization. Nonetheless, some of the results can be compared with field experiments. During SOFEX, two patches were enriched with Fe, one in a high-$[NO_3^-]$, low-$[Si(OH)_4]$ environment and the other in a high-$[NO_3^-]$, high-$[Si(OH)_4]$ environment, with different responses [*Coale et al.*, 2004]. In the low-$[Si(OH)_4]$ case, diatom response to increased [Fe] was somewhat attenuated by Si limitation, while in the high-$[Si(OH)_4]$ case, diatoms dominated the Fe-enhanced bloom. Light attenuation measurements showed that self-shading processes reduced the light penetration in the water column by 50%, which is consistent with our model results.

[38] The failure of the phytoplankton under the present mixing regime to deplete $[NO_3^-]$ to limiting levels in this region, even with abundant Fe, and the role of light limitation in preventing that depletion, are consistent with some earlier predictions derived from field data. *Nelson and Smith* [1991] estimated Sverdrup critical depths in the Southern Ocean as a function of sea surface irradiance and chlorophyll. They then compared those critical depths with mixed layer depths reported from the Southern Ocean in winter, spring and summer and concluded that light/mixing relationships should pose no problem for the initiation and early development of phytoplankton blooms in spring. They concluded, however, that self-shading should keep maximum chlorophyll levels below ~ 1 mg m^{-3} in a 50 m mixed layer, even in midsummer. Those relationships thus suggested that vertical mixing sets a rather modest upper limit on the phytoplankton biomass that can be achieved even when all chemical and biological conditions are ideal for growth. In our simulations with the flexible-composition model, this is exactly what happens once Fe limitation is eliminated by high-dust inputs. Increased chlorophyll levels limit the vertical penetration of PAR in summer, chlorophyll is held below 1 mg m^{-3} for all but a

brief period in midsummer and the resulting light limitation prevents depletion of $[NO_3^-]$ to $<\sim15\ \mu M$.

[39] As noted in section 3.4, the modeling results reported here imply that under present mixing conditions, and with aeolian Fe supplied at the present rate, phytoplankton growth and nutrient utilization are controlled by the interacting effects of Fe limitation and light limitation as proposed by *Sunda and Huntsman* [1997]. They further imply that increasing the Fe supply, either through increased aeolian inputs or by deliberate Fe fertilization, would lead to a system where decreased irradiance in the mixed layer would limit any increase in primary productivity, nutrient drawdown or organic matter export. These conditions may severely constrain the response of the carbon cycle in the Southern Ocean to any increase in Fe supply.

References

Anderson, T. R. (1993), A spectrally averaged model of light penetration and photosynthesis, *Limnol. Oceanogr.*, 38, 1403–1419.
Aumont, O., E. Maier-Reimer, S. Blain, and P. Monfray (2003), An ecosystem model of the global ocean including Fe, Si, P colimitations, *Global Biogeochem. Cycles*, 17(2), 1060, doi:10.1029/2001GB001745.
Blain, S., P. N. Sedwick, F. P. Griffiths, B. Quéguiner, E. Bucciarelli, M. Fiala, P. Pondaven, and P. Tréguer (2002), Quantification of algal requirements in the subantarctic Southern Ocean (Indian sector), *Deep Sea Res., Part II*, 49, 3255–3273.
Boyd, P. W., et al. (2000), A mesoscale phytoplankton bloom in the polar Southern Ocean stimulated by iron fertilization, *Nature*, 407, 695–702.
Boyd, P. W., et al. (2002), Environmental factors controlling phytoplankton processes in the Southern Ocean, *J. Phycol.*, 38, 844–861.
Boyd, P. W., et al. (2004), The decline and fate of an iron-induced subarctic phytoplankton bloom, *Nature*, 428, 549–553.
Brzezinski, M. A. (1985), The Si:C:N ratio of marine diatoms: Interspecific variability and the effect of some environmental variables, *J. Phycol.*, 21, 347–357.
Buesseler, K., J. E. Andrews, S. M. Pike, M. A. Charette, L. E. Goldson, M. Brzezinski, and V. P. Lance (2005), Particle export during the Southern Ocean Iron Experiment (SoFex), *Limnol. Oceanogr.*, 50, 311–327.
Coale, K. H., et al. (1996), A massive phytoplankton bloom induced by an ecosystem scale iron fertilization experiment in the equatorial Pacific Ocean, *Nature*, 383, 511–513.
Coale, K. H., et al. (2004), Southern Ocean Iron Enrichment Experiment: Carbon cycling in high- and low-Si waters, *Science*, 304, 408–414.
De Baar, H. J. W., et al. (2005), Synthesis of eight in-situ iron fertilizations in high nutrient low chlorophyll waters confirms the control by wind mixed layer depth of phytoplankton blooms, *J. Geophys. Res.*, 110, C09S16, doi:10.1029/2004JC002601.
Droop, M. R. (1974), The nutrient status of algal cell in continuous culture, *J. Mar. Biol. Assoc. U.K.*, 54, 825–855.
Droop, M. R. (2003), In defense of the Cell Quota model of micro-algal growth, *J. Plankton Res.*, 25, 103–107.
Falkowski, P. G., R. T. Barber, and V. Smetacek (1998), Biogeochemical controls and feedbacks on ocean primary production, *Science*, 281(5374), 200–206.
Fennel, K., M. R. Abbott, Y. Spitz, H. Y. Richman, and D. M. Nelson (2003), Impact of iron control on phytoplankton production in the modern and glacial Southern Ocean, *Deep Sea Res., Part II*, 50, 833–851.
Fung, I. Y., S. K. Meyn, I. Tegen, S. C. Doney, J. G. John, and J. K. B. Bishop (2000), Iron supply and demand in the upper ocean, *Global Biogeochem. Cycles*, 14, 281–295.
Gao, Y., S. Fan, and J. L. Sarmiento (2003), Aeolian iron input to the ocean through precipitation scavenging: A modeling perspective and its impli-

cation for natural iron fertilization in the ocean, *J. Geophys. Res.*, 108(D7), 4221, doi:10.1029/2002JD002420.
Gaspar, P., Y. Gregories, and J. M. Lefèvre (1990), A simple eddy kinetic energy model for simulation of the oceanic vertical mixing: Test at Station Papa and long term upper ocean study site, *J. Geophys. Res.*, 95, 16,179–16,193.
Gervais, F., U. Riebesell, and M. Y. Gorbunov (2002), Changes in primary productivity and chlorophyll a in response to iron fertilization in Southern Polar Frontal Zone, *Limnol. Oceanogr.*, 47(5), 1324–1335.
Hiscock, M. R., J. Marra, W. O. Smith Jr., R. Goericked, C. Measures, S. Vink, R. J. Olson, H. M. Sosik, and R. T. Barber (2003), Primary productivity and its regulation in the Pacific Sector of the Southern Ocean, *Deep Sea Res., Part II*, 50, 533–558.
Hutchins, D. A., and K. W. Bruland (1998), Iron-limited diatom growth and Si:N uptake ratios in a coastal upwelling regime, *Nature*, 393, 561–564.
Jiang, M., and F. Chai (2004), Iron and silicate regulation of new and export production in the equatorial Pacific: A physical-biological model study, *Geophys. Res. Lett.*, 31, L07307, doi:10.1029/2003GL018598.
Lancelot, C., E. Hannon, S. Becquevort, C. Veth, and J. W. de Baar (2000), Modeling phytoplankton blooms and carbon export production in the Southern Ocean: Dominant controls by light and iron in the Atlantic sector during Austral Spring 1992, *Deep Sea Res., Part I*, 47, 1621–1662.
Martin, J. H. (1990), Glacial-interglacial CO_2 changes: The iron hypothesis, *Paleoceanography*, 5, 1–13.
Matear, R. J., and A. C. Hirst (2003), Long-term changes in dissolved oxygen concentrations in the ocean caused by protracted global warming, *Global Biogeochem. Cycles*, 17(4), 1125, doi:10.1029/2002GB001997.
Michaels, A. F., et al. (1994), Seasonal patterns of ocean biogeochemistry at the U.S. JGOFS Bermuda Atlantic time-series study site, *Deep Sea Res., Part I*, 41, 1013–1038.
Mongin, M., D. M. Nelson, P. Pondaven, M. Brzezinski, and P. Tréguer (2003), Simulation of upper-ocean biogeochemistry with a flexible-composition phytoplankton model: C, N and Si cycling in the western Sargasso Sea, *Deep Sea Res., Part I*, 50, 1445–1480.
Mongin, M., D. M. Nelson, P. Pondaven, and P. Tréguer (2006), Simulation of upper-ocean biogeochemistry with a flexible-composition phytoplankton model: C, N and Si cycling and Fe limitation in the Southern Ocean, *Deep Sea Res., Part II*, 53(5–7), 601–619.
Moore, J. K., S. C. Doney, D. M. Glover, and I. Y. Fung (2002), An intermediate complexity marine ecosystem model for the global domain, *Deep Sea Res., Part II*, 49, 403–462.
Morel, A. (1991), Light and marine photosynthesis: A spectral model with geochemical and climatological implication, *Prog. Oceanogr.*, 26, 263–306.
Nelson, D. M., and W. O. Smith Jr. (1991), Sverdrup revisited: Critical depths, maximum chlorophyll levels, and the control of Southern Ocean productivity by the irradiance-mixing regime, *Limnol. Oceanogr.*, 36(8), 1650–1661.
Nelson, D. M., M. A. Brzezinski, D. E. Sigmon, and V. M. Franck (2001), A seasonal progression of Si limitation in the Pacific sector of the Southern Ocean, *Deep Sea Res., Part II*, 48, 3973–3995.
Nelson, D. M., et al. (2002), Vertical budgets for organic carbon and biogenic silica in the Pacific sector of the Southern Ocean, 1996–1998, *Deep Sea Res., Part II*, 49, 1645–1673.
Petit, J. R., et al. (1999), Climate and atmospheric history of the past 420,000 years from the Vostok ice core, Antarctica, *Nature*, 399, 429–436.
Siegel, D. A., S. C. Doney, and J. A. Yoder (2002), The North Atlantic spring phytoplankton bloom and Sverdrup's critical depth hypothesis, *Science*, 296, 730–733.
Strzepek, R. F., and N. M. Price (2000), Influence of irradiance and temperature on the iron content of the marine diatom Thalassiosira weissflogii (Bacillariophyceae), *Mar. Ecol. Prog. Ser.*, 206, 107–117.
Sunda, W. G., and S. A. Huntsman (1997), Interrelated influence of iron, light and cell size on marine phytoplankton growth, *Nature*, 390, 389–392.
Takeda, S. (1998), Influence of iron availability on nutrient consumption ratio of diatoms in oceanic water, *Nature*, 393, 774–777.

———————————
M. Mongin, ACECRC, Private Bag 80, Hobart, Tasmania 7001, Australia. (mathieu.mongin@acecrc.org.au)
D. M. Nelson, P. Pondaven, and P. Tréguer, Institut Universitaire Européen de la Mer-UMR CNRS 6539, Technopole Brest-Iroise, Place Nicolas Copernic, F-29280 Plouzané, France.